

# Investigation on Breakdown Characteristics of Various Surface Terminal Structures for GaN-Based Vertical P-i-N Diodes

Song Shi, Guanyu Wang, Yingcong Xiang, Chuan Guo, Xing Wang, Yinlin Pu, Huilan Li, Zhixian Li

School of Optoelectronic Engineering, Chongqing University of Posts and Telecommunications, Chongqing, China  
Email: 1764118735@qq.com

**How to cite this paper:** Shi, S., Wang, G.Y., Xiang, Y.C., Guo, C.A., Wang, X., Pu, Y.L., Li, H.L. and Li, Z.X. (2024) Investigation on Breakdown Characteristics of Various Surface Terminal Structures for GaN-Based Vertical P-i-N Diodes. *Journal of Applied Mathematics and Physics*, 12, 554-568.

<https://doi.org/10.4236/jamp.2024.122037>

**Received:** January 24, 2024

**Accepted:** February 26, 2024

**Published:** February 29, 2024

Copyright © 2024 by author(s) and Scientific Research Publishing Inc.  
This work is licensed under the Creative Commons Attribution International License (CC BY 4.0).

<http://creativecommons.org/licenses/by/4.0/>



Open Access

## Abstract

GaN-based vertical P-i-N diode with mesa edge terminal structure due to electric field crowding effect, the breakdown voltage of the device is significantly reduced. This work investigates three terminal structures, including deeply etched, bevel, and stepped-mesas terminal structures, to suppress electric field crowding effects at the device and junction edges. Deeply-etched mesa terminal yields a breakdown voltage of 1205 V, *i.e.*, 89% of the ideal voltage. The bevel-mesa terminal achieves about 89% of the ideal breakdown voltage, while the step-mesa terminal is less effective in mitigating electric field crowding, at about 32% of the ideal voltage. This work can provide an important reference for the design of high-power, high-voltage GaN-based P-i-N power devices, finding a terminal protection structure suitable for GaNPiN diodes to further enhance the breakdown performance of the device and to unleash the full potential of GaN semiconductor materials.

## Keywords

GaN, P-i-N, Mesa Edge Terminal, Electric Field Crowding

## 1. Introduction

Gallium nitride (GaN) is a representative wide-bandwidth semiconductor material, due to its superior material properties (e.g. high electron mobility, high electron saturation velocity, high thermal conductivity, and critical electric field), which are growing concerns [1] [2] [3] [4]. These superior material properties translate into higher breakdown voltage, lower on-resistance, and low power loss. Vertical GaN power devices offer huge advantages. GaN-based devices with low energy consumption, high power density, high operating fre-

quency and high conversion efficiency have been applied to power electronic systems [5] [6] [7]. By increasing the thickness of the drift layer without increasing the size, it can achieve higher breakdown voltage, but it also has a high current, better heat dissipation, smaller chip area, and low dislocation density, which is widely used in the field of electronics and electricity [8]-[14]. Among them, GaN-based vertical P-i-N diodes with high breakdown voltage, low on-resistance, and lower reverse leakage current have been extensively studied, and great progress has been made [15]-[25]. However, destructive breakdown and premature avalanche breakdown occur due to electric field crowding effects at device edges, P-N junction edges, depletion region edges, and electrode edges. To mitigate the electric field at the edge, power devices with improved avalanche breakdown capability have a high breakdown voltage. Edge terminal techniques have been widely used in power devices to reduce the tip electric field by controlling the depletion region of the junction. To reduce the tip electric field at the device edge, device structures with terminal protection have been developed. Various edge terminal techniques have now been employed to mitigate the electric field aggregation effect at the edges of GaN PiN to obtain higher breakdown voltages. These techniques mainly include such as field plates, ion implantation and plasma treatment, mesa etching, etc [10]. It should be noted that these edge terminal techniques do not degrade the forward characteristics and can be used in combination to achieve better device performance.

Mesa etching is a key step in the fabrication of GaN-based devices to isolate neighboring devices, and due to its simplicity, mesa etching terminal structures are very popular in GaN-based vertical P-i-N diodes. Recently, Fukushima [26] and others designed deeply etched mesa structures to alleviate the electric field crowding at the device edges, where the deeper the mesa, the more relaxed the edge electric field. In addition to the common vertical mesa structure, a negative-angle mesa structure is usually obtained in actual device fabrication. However, the appropriate P<sup>+</sup>-GaN doping concentration and bevel angle can also mitigate the P-N junction edge electric field and transfer the tip electric field to the inside [27] [28] [29]. Stepped-mesa edge terminal has been reported to increase the device breakdown voltage of GaN power devices [30]. For structures with a stepped mesa, the parameters such as width, depth, and number of steps play an important role.

Therefore, in order to make the breakdown voltage close to that of an ideal parallel-plane device. In this thesis, we investigate three mesa-based edge terminal techniques using SILVACO TCAD, *i.e.*, deeply-etched mesa, beveled mesa, stepped mesa edge terminal. With the starting point that vertical GaN PiN power diodes can fundamentally break through the breakdown voltage of traditional planar-type PiN diodes, the terminal protection technology at the present stage is discussed in detail and analyzed with simulation results, to find the terminal protection structure applicable to GaN PiN diodes, to further enhance the breakdown performance of the devices and to fully release the potential of GaN semiconductor materials.

## 2. Simulation Results

### 2.1. Prototype Device Structure and Parameters

The different GaN-based vertical P-i-N diode structures have been implemented, calibrated and simulated in SILVACO TCAD. **Figure 1** shows the ideal parallel planar GaN P-i-N diode structure. These include a P<sup>+</sup>-GaN layer with a thickness of 500 nm and a doping concentration of  $1 \times 10^{19} \text{ cm}^{-3}$ ; an N<sup>-</sup>-GaN layer with a thickness of 10  $\mu\text{m}$  and a doping concentration of  $2 \times 10^{16} \text{ cm}^{-3}$ ; and an N<sup>+</sup>-GaN layer with a thickness of 2  $\mu\text{m}$  and a doping concentration of  $2 \times 10^{18} \text{ cm}^{-3}$ . It should be noted that the high concentration doped P<sup>+</sup>-GaN region is approximated as a one-sided step junction due to its narrow space charge region. The breakdown voltage is almost independent of the thickness of the P<sup>+</sup>-GaN layer, and the thickness of the P<sup>+</sup>-GaN layer of the actual device is generally smaller, hence the simulation structure proposed in this section is also designed as a very thin layer. The material parameters of the GaN used for simulation and the model and its parameters are shown in **Table 1**. In addition to the above models, there are also the bandgap narrowing model (BGN), the Farahm and modified Caughey-Thomas model (FMCT), the nitride high-field mobility model (GANSAT.N), and the Fermi-Dirac statistical model (Fermi-Dirac).

**Table 1.** Material and model parameters for GaN.

Material/Model	Property	Values
GaN	Bandgap (eV)	3.43
	Electron affinity (eV)	4.1
	Dielectric constant	8.9
	Effective Conduction Band Density of states ( $\text{cm}^{-3}$ )	$2.24 \times 10^{18}$
	Effective Valence Band Density of states ( $\text{cm}^{-3}$ )	$2.51 \times 10^{19}$
Impact Ionization	$a_{n1/2}$ ( $\text{cm}^{-1}$ )	$2.52 \times 10^8$
	$b_{n1/2}$ (V/cm)	$3.41 \times 10^7$
	$a_{p1/2}$ ( $\text{cm}^{-1}$ )	$5.37 \times 10^6$
	$b_{p1/2}$ (V/cm)	$1.96 \times 10^7$
Incomplete Ionization	Donor Activation Energy ( $\Delta E_D$ ) (meV)	17
	$\alpha_n$ (eV.cm)	$3.4 \times 10^{-9}$
	Acceptor Activation Energy ( $\Delta E_A$ ) (meV)	240
	$\alpha_p$ (eV.cm)	$1.15 \times 10^{-9}$
SRH Recombination	Electron Lifetime ( $\tau_n$ )	$1.2 \times 10^{-8}$
	Hole Lifetime ( $\tau_p$ )	$1.2 \times 10^{-8}$
Auger Recombination	Electron Coefficient ( $\text{cm}^{-3}\cdot\text{s}$ )	$2.8 \times 10^{-31}$
	Hole Coefficient ( $\text{cm}^{-3}\cdot\text{s}$ )	$9.9 \times 10^{-32}$

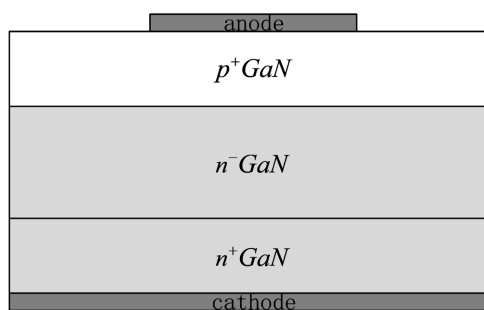


**Figure 1.** Ideal parallel plane GaN-based vertical P-i-N diode structure.

## 2.2. Deeply-Etched Mesa Terminal Structure

As shown in **Figure 2** shows the schematic cross-section of the GaN-based vertical P-i-N diode used for simulation. Simulation studies are carried out on device structures with etching depths ranging from  $0.5 \mu\text{m}$  to  $7 \mu\text{m}$  (referring to the etching depth of the n-drift region), keeping other parameters constant. As shown in **Figure 3**, the breakdown voltage increases almost linearly with the depth of the mesa etching. With the increase in the etching depth of the mesa, the breakdown voltage gradually approaches the ideal parallel plane breakdown voltage. For deep etch  $T = 7 \mu\text{m}$ , the device breakdown voltage is 1205 V, which is 97% of the breakdown voltage of an ideal parallel-plane device.

As **Figure 4** demonstrates the electric field distribution when avalanche breakdown occurs in devices with GaN-based vertical P-i-N diode etching depths of  $T = 1 \mu\text{m}$ ,  $3 \mu\text{m}$  and  $5 \mu\text{m}$ , respectively, it can be observed that the electric field aggregation effect obviously occurs at the edge of the device, and with the increase of the etching depth attenuating the tip electric field at the edge to make the electric field homogeneous and sparse, and for the devices with deeper etching of the mesa surface, the distribution of the electric field is more homogeneous, especially at the edges.

One-dimensional electric field distributions in the perpendicular direction from the center of the GaN-based vertical P-i-N diode junction to the edge were extracted for different etching depths, as shown in **Figure 5**. At shallow etching depths, the device edge electric field crowding is very significant, and the peak electric field reaches up to  $3.6 \text{ MV/cm}$  at etching depth  $T = 0.5 \mu\text{m}$ , leading to premature breakdown at the edge, at which time the center of the P-N junction is still far from reaching the GaN critical electric field of  $3.3 \text{ MV/cm}$ . When the etching depth  $T = 4 \mu\text{m}$ , avalanche breakdown occurs when the electric field strength at the center of the P-N junction is comparable to the electric field at the edge, which is almost equal to the GaN critical electric field of  $3.3 \text{ MV/cm}$ , and it can be assumed that the breakdown occurs at the same time. When the etching depth  $T > 5 \mu\text{m}$ , the avalanche breakdown occurs when the center field of the P-N junction is slightly larger than the edge field. When the etching depth is  $T = 7 \mu\text{m}$ , with the same condition, the electric field at the tip edge is very small and much smaller than that at the center of the P-N junction, and at this

time, the breakdown voltage and electric field distribution are close to those of an ideal parallel planar GaN-based vertical P-i-N diode.

These results show that in vertical mesa etching, the deeper the etching depth, the smaller and further away from the center of the P-N junction the electric field at the tip of the device edge, the more uniform the electric field inside the device, the less prone to premature breakdown at the edge, and the larger the breakdown voltage. Therefore, in the design of a vertical mesa etching terminal structure, the mesa is etched to a greater depth than the edge of the depletion region, and the breakdown voltage can be raised to a level close to the ideal parallel planar structure. Moreover, this terminal method has a simple process step, but it is necessary to deposit a passivated dielectric layer on mesa terminal structure in order to suppress the leakage current caused by the plasma damage of etching.

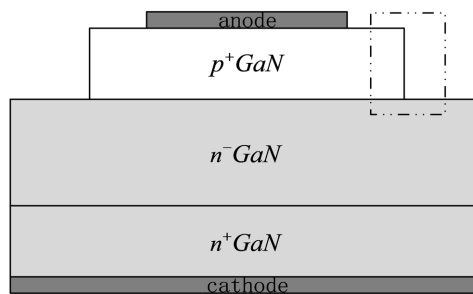


Figure 2. Deeply-etched mesa edge terminal.

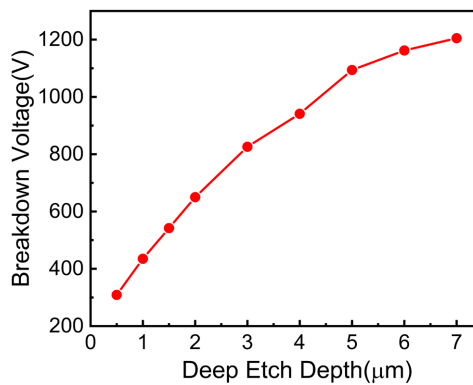


Figure 3. Breakdown voltage of GaN-based vertical P-i-N diode with different etched depths.

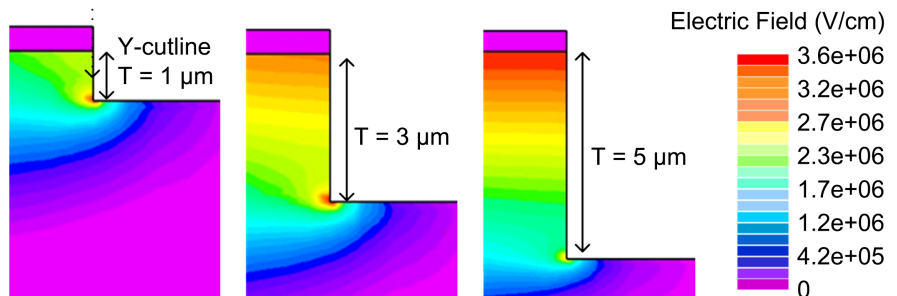
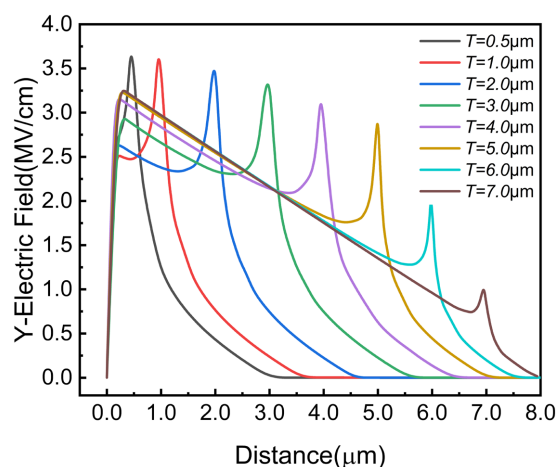


Figure 4. Electric field distributions of devices with  $T = 1 \mu\text{m}$ ,  $T = 3 \mu\text{m}$  and  $T = 5 \mu\text{m}$  when avalanche breakdown occurs.



**Figure 5.** Electric field distributions along the vertical direction (Y-cutline).

### 2.3. Bevel Mesa Terminal Structure

There are two general types of bevel mesa structures, positive bevel angle and negative bevel angle. In practice, negative bevel angle mesa terminal structures are easier to realize and are often used in wide-band semiconductor devices. In the bevel mesa terminal structure simulation, the P-N junction edges are etched at an angle, and the mesa bevel angle is increased from  $10^\circ$  to  $80^\circ$ . In addition, the breakdown voltage of this terminal structure is extremely sensitive to the doping concentration of the  $P^+$ -GaN layer, and the doping concentrations of the  $P^+$ -GaN layer of  $1 \times 10^{18} \text{ cm}^{-3}$  and  $5 \times 10^{18} \text{ cm}^{-3}$  were also simulated during the simulation process. In **Figure 6** a schematic cross-sectional view of a bevel mesa terminal structure for simulation is shown.

Structures with  $P^+$ -GaN layer doping concentrations of  $N_a = 1 \times 10^{18} \text{ cm}^{-3}$ ,  $5 \times 10^{18} \text{ cm}^{-3}$ , and  $1 \times 10^{19} \text{ cm}^{-3}$  were simulated under non-pass-through conditions in order to investigate the effect of doping concentration variations on the terminal structure of the bevel mesa. It should be noted that the doping concentration of the  $P^+$ -GaN layer should not be too low in order to form good ohmic contacts. In **Figure 7**, the breakdown voltages of GaN-based vertical P-i-N diodes at different bevel angles for each  $P^+$ -GaN layer doping concentration are shown. For all  $P^+$ -GaN layer doping concentrations of the bevel mesa terminal structure, the breakdown voltage decreases with decreasing  $\theta$ , eventually remaining almost constant at small angles. However, at high-concentration doping of the  $P^+$ -GaN layer with  $N_a = 1 \times 10^{19} \text{ cm}^{-3}$ , the breakdown voltage decreases faster and reaches a lower value of 450 V at small angles, whereas at low-concentration doping of the  $P^+$ -GaN layer with  $N_a = 1 \times 10^{18} \text{ cm}^{-3}$  a larger breakdown voltage of 850 V can still be obtained at small angles. The device has the highest breakdown voltage of 1160 V when  $\theta = 80^\circ$  and  $N_a = 1 \times 10^{18} \text{ cm}^{-3}$ , when the device is also close to the ideal parallel plane structure.

The electric field distribution at a reverse bias voltage of 350 V for  $P^+$ -GaN doping concentration  $N_a = 1 \times 10^{19} \text{ cm}^{-3}$  at angles of  $10^\circ$ ,  $40^\circ$ , and  $70^\circ$ , respectively,

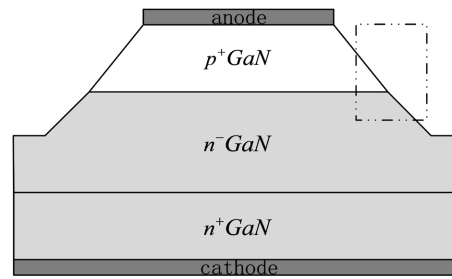


**Figure 6.** Beveled mesa edge terminal.

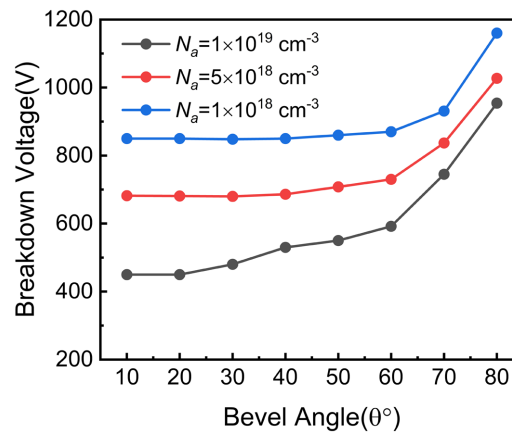


**Figure 7.** Breakdown voltage of GaN P-i-N diode with the bevel angle for  $N_a = 1 \times 10^{18} \text{ cm}^{-3}$ ,  $5 \times 10^{18} \text{ cm}^{-3}$  and  $1 \times 10^{19} \text{ cm}^{-3}$ .

was extracted in order to better understand the effect of the angle of the terminal of the bevel mesa on the breakdown voltage, as shown in **Figure 8**. At a small bevel angle  $\theta = 10^\circ$ , a tip electric field is generated at the edge P-N junction due to the smaller width of the depletion region on the beveled surface, which can lead to premature breakdown. As the bevel angle gradually increases, the depletion region on the bevel sidewall surface extends toward the interior, which mitigates the tip electric field at the junction edge, resulting in an increase in the breakdown voltage. At a large bevel angle  $\theta = 70^\circ$ , the surface depletion region boundary extends further inward, and the electric field distribution of the device is more uniform in both the vertical and horizontal directions, which is then closer to the ideal parallel plane structure electric field distribution.

In order to further understand the effect of the bevel mesa terminal on the electric field at different angles, the one-dimensional electric field distributions of GaN-based vertical P-i-N diodes at different bevel angles in the vertical and horizontal directions were extracted, as shown in **Figure 9**. It can be seen that both vertical and horizontal maximum electric fields at the P-N junction edge increase with decreasing angle. As the bevel angle  $\theta$  gradually increases from  $10^\circ$  to  $80^\circ$ , the electric field strength in the X direction decreases from a maximum of 3.6 MV/cm to 1.8 MV/cm, and the electric field strength in the Y direction decreases from a maximum of 3.3 MV/cm to 1.7 MV/cm.

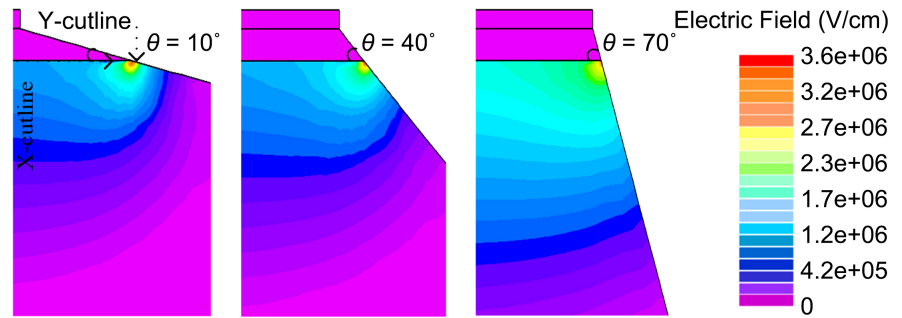


**Figure 8.** Electric field distributions of devices with  $\theta = 10^\circ$ ,  $\theta = 40^\circ$  and  $\theta = 70^\circ$  at reverse bias of 350 V.

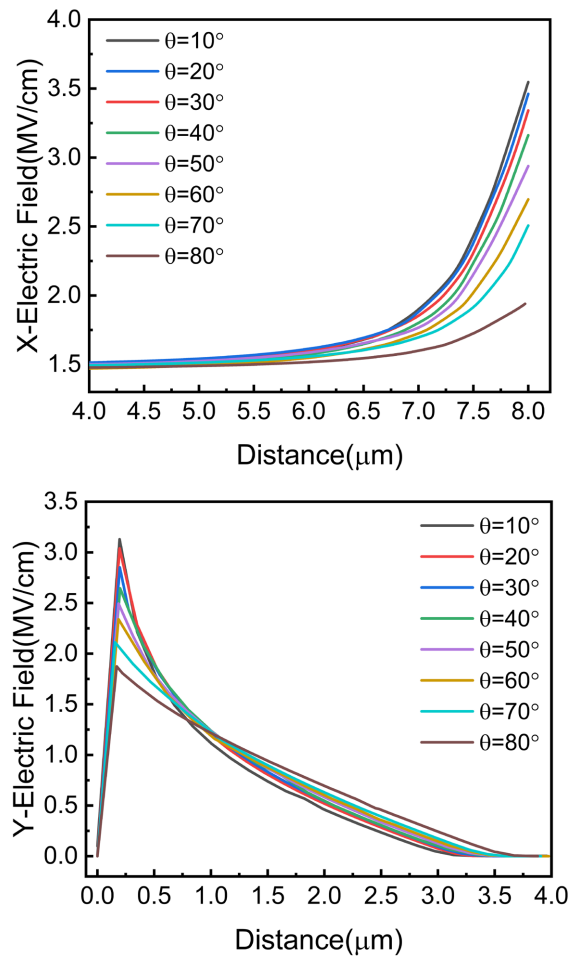


**Figure 9.** Electric field distributions along the X-cutline and Y-cutline.

It is finally concluded that the doping concentration and bevel angle of P<sup>+</sup>-GaN in the bevel mesa terminal structure have a crucial effect on the breakdown voltage. At relatively large bevel angles, the devices have a more uniform electric field and a high breakdown voltage. Also at small angles, by reducing the doping concentration in the P<sup>+</sup>-GaN region, the device can be brought to a better level of breakdown voltage. These results are instructive for designing GaN



PiN diodes with bevel mesa terminal structures.

#### 2.4. Stepped-Mesa Terminal Structure

The key parameters of the step mesa terminal include step width ( $W$ ), step depth ( $D$ ), and number of steps. In the simulations, combinations of ( $W, D$ ) of ( $0.5 \mu\text{m}, 0.5 \mu\text{m}$ ) and ( $0.5 \mu\text{m}, 1.0 \mu\text{m}$ ) and ( $1.0 \mu\text{m}, 1.0 \mu\text{m}$ ), respectively, were investigated, where the values of all three combinations were expressed in  $\mu\text{m}$ . The drift layer was etched into a step type to disperse the electric field aggregation effect. P-N junction interface at  $500 \text{ nm}$ , where  $n$  is the number of step steps. A schematic cross-section of the step mesa terminal structure used for the simulation is shown in **Figure 10**.

**Figure 11** shows the breakdown voltages for three different ( $W, D$ ) combinations at different numbers of steps. At the same number of steps, the device has the highest breakdown voltage for ( $W, D$ ) = ( $0.5 \mu\text{m}, 1.0 \mu\text{m}$ ), respectively. The results of the simulation show that the smaller the width  $W$  and the larger the depth  $D$  of the steps, the higher the breakdown voltage. This is due to the fact that the drift layer is etched as a step type, and the electric field is forced to spread in the vertical direction instead of the lateral direction. The smaller the  $W$ , the larger the  $D$ , which means that more material is removed from the transverse direction, and the electric field must spread vertically to the interior of the drift layer due to the lack of material in the transverse direction. The peak

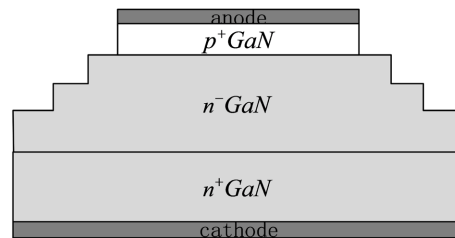


**Figure 10.** Stepped-mesa edge terminal.

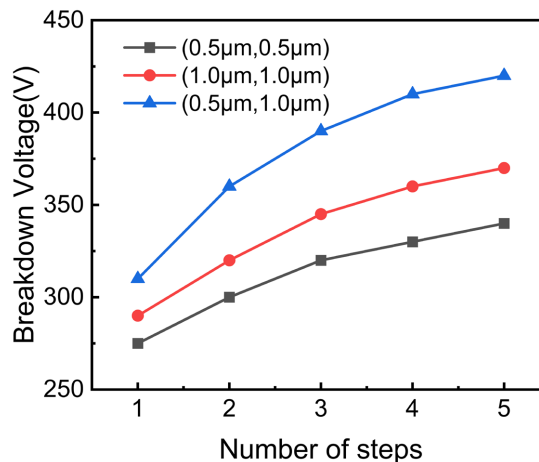


**Figure 11.** Breakdown voltage of GaN-based vertical P-i-N diode with different  $W, D$  and number of steps.

electric field will be shifted from the center of the P-N junction to the step behind it and spread to the inside of the drift layer. The combination of a small width  $W$  and a large depth  $D$ , results in a higher breakdown voltage because it can withstand a higher voltage inside than at the edge. In addition, in all three cases, the increase in the number of steps will result in the edge electric field distribution being more uniform, and the breakdown voltage will increase.

These trends can be explained in **Figure 12**, where the step mesa structure disperses the peak electric field at each step and reduces the overall electric field at the center of the P-N junction. The lateral electric field distribution of the figure shows that the step mesa terminals have multiple localized smaller peaks of the electric field at the etched corners.

As shown in **Figure 13**, compared to the peak electric field at the edge of the p-n junction, the localized peak electric field distribution in the X-direction decreases to 3.5 MV/cm, 1.9 MV/cm, 0.8 MV/cm, and 0.3 MV/cm after passing through the four-step mesa, and the localized peak electric field in the Y-direction decreases to 2.4 MV/cm, 1.9 MV/cm, 0.9 MV/cm, and 0.3 MV/cm. These additional electric field peaks help to mitigate the overall electric field aggregation at the edges of the P-N junction, thereby increasing the breakdown voltage. In addition, too much depth reduces the number of achievable steps, which may have a negative impact on the breakdown voltage. However, if the width can be minimized as much as possible, this will also help to improve the breakdown voltage.

It can be concluded that as the number of steps increases, more local electric field peaks are generated at the device edge to alleviate the electric field concentration effect at the center of the P-N junction, thus increasing the device breakdown voltage. When  $(W, D) = (0.5 \mu\text{m}, 1.0 \mu\text{m})$  and the number of steps is 5, the breakdown voltage is up to 430 V, which is much smaller than the one of the

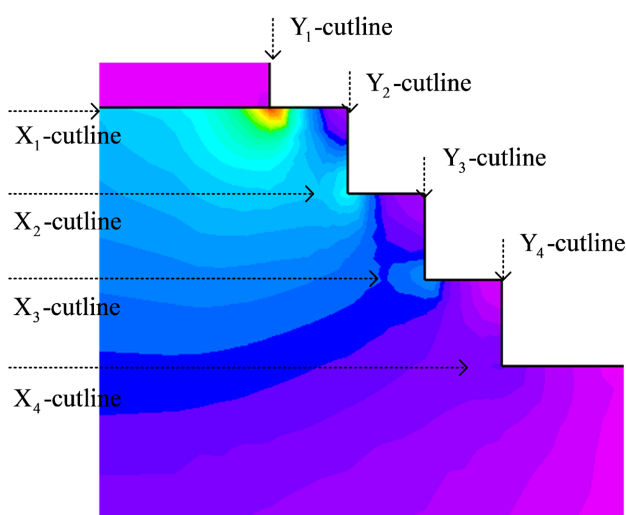


**Figure 12.** Electric field distributions of devices with  $W = 0.5 \mu\text{m}$ ,  $D = 1.0 \mu\text{m}$  and number of steps = 4 at reverse bias of 300 V.

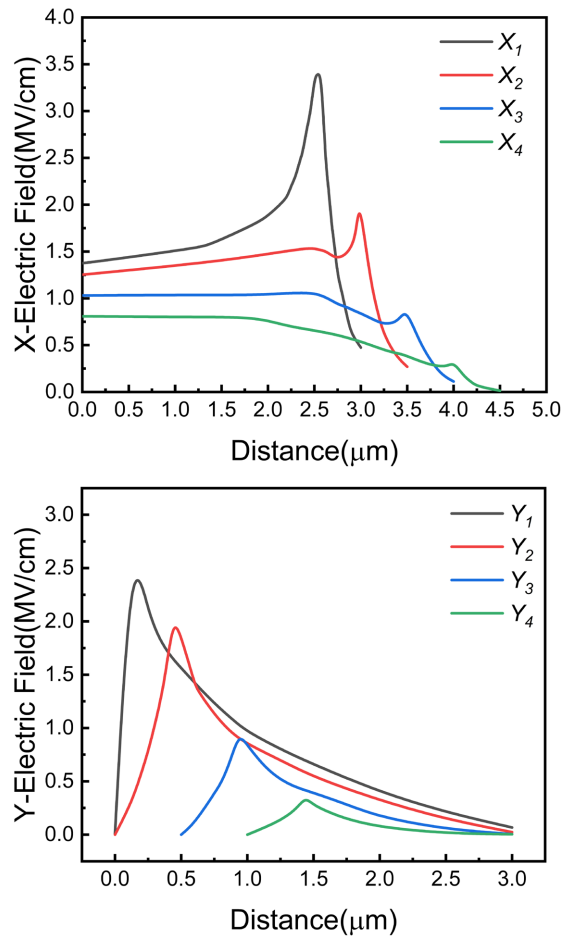


**Figure 13.** Electric field distributions along the  $X_1$ - $X_4$  cutline and  $Y_1$ - $Y_4$  cutline.

ideal parallel planar structure, and is about 32% of the breakdown voltage of the ideal parallel planar structure, which is worse than that of the other terminal structures. In addition, the maximum number of steps for the device will be drift layer thickness dependent, but the more steps on the mesa top, the more fabrication steps there will be, which may lead to more etch damage, more fabrication cost and less device reliability. Therefore, the choice of the number of mesa steps is a trade-off between breakdown voltage, fabrication cost, and reliability.

### 3. Results and Discussion

The performance of GaN-based vertical P-i-N diodes prepared using different terminal protection techniques was compared, as shown in **Figure 14**. Notably, the forward  $I$ - $V$  characteristics of these different terminal structure devices are similar to those of the ideal parallel plane structure, which means that these terminal structures do not degrade the forward conduction performance. In addition, these terminal structures have different parameters, and the breakdown voltage may also be further enhanced by changing these parameters. For example, the breakdown voltage of a bevel mesa terminal structure with a tilt angle

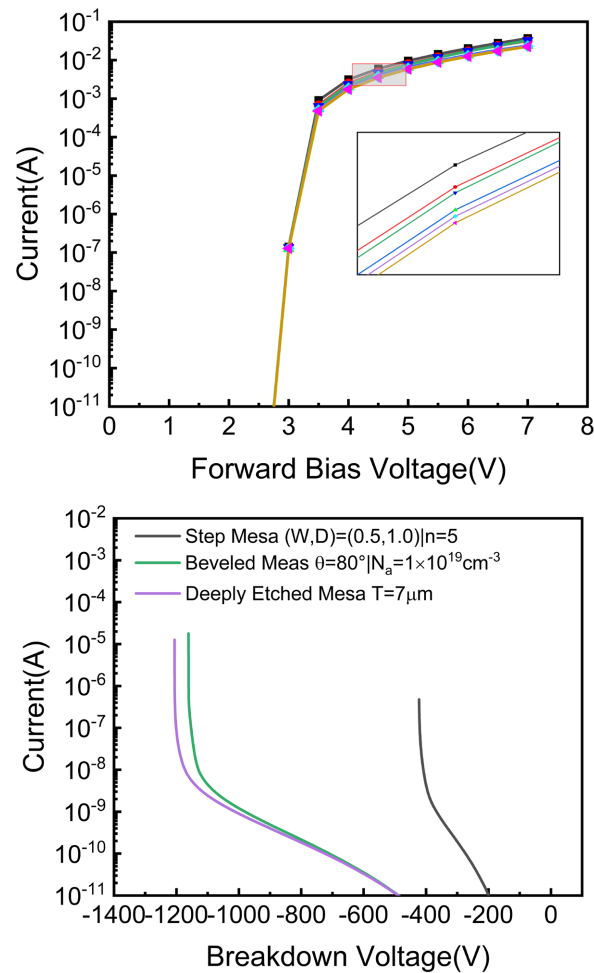


**Figure 14.** Forward  $I$ - $V$  characteristics and reverse  $I$ - $V$  characteristics of different edge terminal structures.

$\theta = 40^\circ$  and a P<sup>+</sup>-GaN layer doping concentration  $N_a = 1 \times 10^{19} \text{ cm}^{-3}$  having a field plate is 1055 V, which is lower than the breakdown voltage of a bevel mesa terminal structure without a field plate with a tilt angle  $\theta = 80^\circ$  and a P<sup>+</sup>-GaN layer doping concentration  $N_a = 1 \times 10^{18} \text{ cm}^{-3}$  of 1060 V. This does not mean that the field-plate terminal structure is inferior to the structure without field-plate terminal, since other parameters itself are quite important.

**Table 2** summarizes the maximum breakdown voltages for each terminal technique in this structure. Devices with deeply etched mesa show large breakdown voltages, close to those of ideal parallel-plane devices. These terminal techniques should be considered in addition to the enhanced breakdown voltage, and the fabrication process for each terminal technique should be considered. Bevel mesa, step mesa, and deeply-etched mesa terminals depend on control of the dry etching process. Whereas both surface burrs and roughness of the field plate metal may lead to electric field spikes or long-term reliability problems in high-voltage devices, this problem is now generally addressed by growing the dielectric under the field plate.

**Table 2.** Breakdown voltage for each edge terminal technologies.

Edge terminal technology	Breakdown voltage (V)/%	Device parameter
Deeply Etched Meas	1205 (92%)	$T = 7 \mu\text{m}$
Beveled Meas	1160 (89%)	$\theta = 80^\circ, N_d = 1 \times 10^{19} \text{cm}^{-3}$
Step Meas	425 (32%)	$W = 0.5 \mu\text{m}, D = 1.0 \mu\text{m}, n = 5$

It is worth noting that the simulation work done in this section uses only  $n^-$ -GaN drift layers with a doping concentration of  $N_d = 2 \times 10^{16} \text{cm}^{-3}$  and a thickness of  $10 \mu\text{m}$ , with the main purpose of demonstrating the protection capability of these terminal techniques. When the doping concentration drift layer is decreased to  $N_d = 1 \times 10^{16} \text{cm}^{-3}$  and the thickness is increased to  $20 \mu\text{m}$ , the breakdown voltage can be increased up to  $2500 \text{V}$ . When the doping concentration drift layer is decreased to  $N_d = 5 \times 10^{15} \text{cm}^{-3}$  and the thickness is increased to  $20 \mu\text{m}$ , the breakdown voltage can be increased up to  $3800 \text{V}$ .

#### 4. Conclusions

This work has presented a simulation analysis of edge terminal protection technologies, which have been a hot research topic in recent years, to demonstrate the protection reliability of these terminal technologies. In SILVACO TCAD simulations, three types of mesa edge terminal structures for GaN-based vertical P-i-N diode be designed, modeled, and fully investigated, including deeply-etched mesa, bevel mesa, step mesa. The results show that these terminal structures can alleviate the electric field crowding at the junction edges and improve the breakdown voltage. For deeply-etched mesa terminal structures, the device breakdown voltage increases linearly with countertop etching depth. For the bevel mesa terminal structure, the breakdown voltage decreases with decreasing angle  $\theta$  for all  $P^+$ -GaN layer doping concentrations, eventually remaining almost constant at small angles. For a step mesa terminal structure, the smaller the width  $W$  and the greater the depth  $D$  of the steps, the greater the breakdown voltage. Among these three edge terminal structures, the breakdown voltages of the deeply-etched mesa terminal structures is close to those of the ideal parallel-plane devices, reaching 92% and 94% of their ideal breakdown voltages, respectively, whereas the bevel mesa terminal structure is 89% of the ideal breakdown voltage and the step mesa terminal structure is only 32% of the ideal breakdown voltage. In future research, the device breakdown voltage can be further improved by varying the thickness of the drift layer.

#### Conflicts of Interest

The authors declare no conflicts of interest regarding the publication of this paper.

#### References

- [1] Zhang, Y., Dadgar, A. and Palacios, T. (2018) Gallium Nitride Vertical Power De-

- vices on Foreign Substrates: A Review and Outlook. *Journal of Physics D: Applied Physics*, **51**, Article 27. <https://doi.org/10.1088/1361-6463/aac8aa>
- [2] Flack, T.J., Pushpakaran, B.N. and Bayne, S.B. (2016) GaN Technology for Power Electronic Applications: A Review. *Journal of Electronic Materials*, **45**, 2673-2682. <https://doi.org/10.1007/s11664-016-4435-3>
- [3] Chowdhury, S. and Mishra, U.K. (2013) Lateral and Vertical Transistors Using the AlGaIn/GaN Heterostructure. *IEEE Transactions on Electron Devices*, **60**, 3060-3066. <https://doi.org/10.1109/TED.2013.2277893>
- [4] Amano, H., Baines, Y., Beam, E., et al. (2018) The 2018 GaN Power Electronics Roadmap. *Journal of Physics D: Applied Physics*, **51**, Article No. 16. <https://doi.org/10.1088/1361-6463/aaaf9d>
- [5] Zhang, Y. and Palacios, T. (2020) (Ultra)Wide-Bandgap Vertical Power FinFETs. *IEEE Transactions on Electron Devices*, **67**, 3960-3971. <https://doi.org/10.1109/TED.2020.3002880>
- [6] Roccaforte, F., Greco, G., Fiorenza, P. and Iucolano, F. (2019) An Overview of Normally-Off GaN-Based High Electron Mobility Transistors. *Materials*, **12**, Article 1599. <https://doi.org/10.3390/ma12101599>
- [7] Ding, X., Zhou, Y. and Cheng, J. (2019) A Review of Gallium Nitride Power Device and Its Applications in Motor Drive. *CES Transactions on Electrical Machines and Systems*, **3**, 54-64. <https://doi.org/10.30941/CESTEMS.2019.00008>
- [8] Chowdhury, S., Swenson, B.L., Mishra, U.K. and Wong, M.H. (2013) Current Status and Scope of Gallium Nitride-Based Vertical Transistors for High-Power Electronics Application. *Semiconductor Science and Technology*, **28**, Article No. 7. <https://doi.org/10.1088/0268-1242/28/7/074014>
- [9] Zhang, Y., Sun, M., Liu, Z., et al. (2013) Electrothermal Simulation and Thermal Performance Study of GaN Vertical and Lateral Power Transistors. *IEEE Transactions on Electron Devices*, **60**, 2224-2230. <https://doi.org/10.1109/TED.2013.2261072>
- [10] Anderson, T.J., Greenlee, J.D., Feigelson, B.N., et al. (2016) Improved Vertical GaN Schottky Diodes with Ion Implanted Junction Termination Extension. *ECS Journal of Solid State Science and Technology*, **5**, Article No. 6. <https://doi.org/10.1149/2.0251606jss>
- [11] Tanaka, N., Hasegawa, K., Yasunishi, K., et al. (2015) 50 A Vertical GaN Schottky Barrier Diode on a Free-Standing GaN Substrate with Blocking Voltage of 790 V. *Applied Physics Express*, **8**, Article No. 7. <https://doi.org/10.7567/APEX.8.071001>
- [12] Horii, T., Miyazaki, T. and Saito, Y. (2009) High-Breakdown-Voltage GaN Vertical Schottky Barrier Diodes with Field Plate Structure. *Materials Science Forum*, **615-617**, 963-966. <https://doi.org/10.4028/www.scientific.net/MSF.615-617.963>
- [13] Disney, D., Nie, H. and Edwards, A. (2013) Vertical Power Diodes in Bulk GaN. 2013 25th *International Symposium on Power Semiconductor Devices and IC's (ISPSD)*, Kanazawa, 26-30 May 2013, 5962. <https://doi.org/10.1109/ISPSD.2013.6694455>
- [14] Kizilyalli, I.C., Edwards, A.P. and Aktas, O. (2014) Vertical Power p-n Diodes Based on Bulk GaN. *IEEE Transactions on Electron Devices*, **62**, 414-422. <https://doi.org/10.1109/TED.2014.2360861>
- [15] Nomoto, K., Hatakeyama, Y., Katayose, H., et al. (2011) Over 1.0 kV GaN p-n Junction Diodes on Free-Standing GaN Substrates. *Physica Status Solidi (A)*, **208**, 1535-1537. <https://doi.org/10.1002/pssa.201000976>

- [16] Kozodoy, P., Ibbetson, J.P., Marchand, H., et al. (1998) Electrical Characterization of GaN p-n Junctions with and without Threading Dislocations. *Applied Physics Letters*, **73**, 975-977. <https://doi.org/10.1063/1.122057>
- [17] Hatakeyama, Y., Nomoto, K., Kaneda, N., et al. (2011) Over 3.0 GW/cm<sup>2</sup> Figure-of-Merit GaN p-n Junction Diodes on Free-Standing GaN Substrates. *IEEE Electron Device Letters*, **32**, 1674-1676. <https://doi.org/10.1109/LED.2011.2167125>
- [18] Hatakeyama, Y., Nomoto, K. and Terano, A.L. (2013) High-Breakdown-Voltage and Low-Specific-on-Resistance GaN p-n Junction Diodes on Free-Standing GaN Substrates Fabricated through Low-Damage Field-Plate Process. *Japanese Journal of Applied Physics*, **52**, Article No. 2R. <https://doi.org/10.7567/JJAP.52.028007>
- [19] Kizilyalli, I.C., Edwards, A.P., Nie, H., et al. (2013) 3.7 kV Vertical GaN PN Diodes. *IEEE Electron Device Letters*, **35**, 247-249. <https://doi.org/10.1109/LED.2013.2294175>
- [20] Kizilyalli, I.C., Edwards, A.P., Nie, H., et al. (2014) 400-A (Pulsed) Vertical GaN p-n Diode with Breakdown Voltage of 700 V. *IEEE Electron Device Letters*, **35**, 654-656. <https://doi.org/10.1109/LED.2014.2319214>
- [21] Kizilyalli, I.C., Prunty, T. and Aktas, O. (2015) 4-kV and 2.8-mΩ-cm<sup>2</sup> Vertical GaN p-n Diodes with Low Leakage Currents. *IEEE Electron Device Letters*, **36**, 1073-1075. <https://doi.org/10.1109/LED.2015.2474817>
- [22] Hu, Z., Nomoto, K., Song, B., et al. (2015) Near Unity Ideality Factor and Shockley-Read-Hall Lifetime in GaN-on-GaN p-n Diodes with Avalanche Breakdown. *Applied Physics Letters*, **107**, Article 243501. <https://doi.org/10.1063/1.4937436>
- [23] Dickerson, J.R., Allerman, A.A., and Bryant, B.N. (2016) Vertical GaN Power Diodes with a Bilayer Edge Termination. *IEEE Transactions on Electron Devices*, **63**, 419-425. <https://doi.org/10.1109/TED.2015.2502186>
- [24] Ohta, H., Kaneda, N., Horikiri, F., et al. (2015) Vertical GaN p-n Junction Diodes with High Breakdown Voltages over 4 kV. *IEEE Electron Device Letters*, **36**, 1180-1182. <https://doi.org/10.1109/LED.2015.2478907>
- [25] Ohta, H., Hayashi, K., Horikiri, F., et al. (2018) 5.0 kV Breakdown-Voltage Vertical GaN p-n Junction Diodes. *Japanese Journal of Applied Physics*, **57**, Article No. 4S. <https://doi.org/10.7567/JJAP.57.04FG09>
- [26] Fukushima, H., Usami, S., Ogura, M., et al. (2019) Vertical GaN p-n Diode with Deeply Etched Mesa and the Capability of Avalanche Breakdown. *Applied Physics Express*, **12**, Article No. 2. <https://doi.org/10.7567/1882-0786/aafdb9>
- [27] Maeda, T., Narita, T., Ueda, H., et al. (2019) Design and Fabrication of GaN p-n Junction Diodes with Negative Beveled-Mesa Termination. *IEEE Electron Device Letters*, **40**, 941-944. <https://doi.org/10.1109/LED.2019.2912395>
- [28] Maeda, T., Narita, T. and Ueda, H. (2018) Parallel-Plane Breakdown Fields of 2.8-3.5 MV/cm in GaN-on-GaN p-n Junction Diodes with Double-Side-Depleted Shallow Bevel Termination. *IEEE International Electron Devices Meeting (IEDM)*. San Francisco, 1-5 December 2018, 30.1.1-30.1.4. <https://doi.org/10.1109/IEDM.2018.8614669>
- [29] Zeng, K. and Chowdhury, S. (2020) Designing Beveled Edge Termination in GaN Vertical p-i-n Diode-Bevel Angle, Doping, and Passivation. *IEEE Transactions on Electron Devices*, **67**, 2457-2462. <https://doi.org/10.1109/TED.2020.2987040>
- [30] Yates, L., Gunning, B.P., Crawford, M.H., et al. (2022) Demonstration of > 6.0-kV Breakdown Voltage in Large Area Vertical GaN p-n Diodes with Step-Etched Junction Termination Extensions. *IEEE Transactions on Electron Devices*, **69**, 1931-1937. <https://doi.org/10.1109/TED.2022.3154665>